Shearing x-ray interferometer with an x-ray prism and its improvement

Yoshiki Kohmura, Hidekazu Takano, Kentaro Uesugi, Yoshio Suzuki, Tetsuya Ishikawa
SPring-8, 1-1-1, Kouto, Mikazuki, Sayo-gun, Hyogo, 679-5198, Japan

Abstract

A wave-front dividing interferometer was devised in which half of a highly spatially coherent beam deflected by an x-ray prism is overlapped with another half. By placing the samples in the two beams and the x-ray imaging detector closely downstream of the sample, the differential phase of the sample is recorded on the imaging detector. The separation of the two paths at the sample plane, the amount of shear, was approximately 2 μm in the present experiment. This is easily controllable by changing the distance between the sample and the imaging detector. Phase retrieval using the fringe scanning method was successfully demonstrated for various kinds of weakly absorbing samples.

1. INTRODUCTION

The various methods for phase retrieval are reported for the scattered / diffracted x-rays [1,2] and the trasmitted x-rays [3,4]. The interferometers, using the coherent superposition of transmitted and reference beams, offer the most direct method for unique retrieval of the phase. The crystal Bonse-Hart interferometers (usually as amplitude dividing interferometers) are widely used for the phase retrieval in the hard x-rays [5,6]. Although a shearing geometry has also been attempted [7], the narrow angular acceptance of the crystal optics limits the spatial resolution. In this paper, we will show that the wave-front division using an x-ray prism [8,9] can be used for an x-ray shearing interferometer without significant angular windows and with a better spatial resolution.

2. EXPERIMENTAL SETUP

To obtain a high spatial coherence demanded for the wave-front dividing interferometer, a 250 m long beamline with an undulator source, BL20XU, of SPring-8 was utilized [9]. Monochromatic x-rays at 12.4 keV (λ= 1 Å) through a silicon monochromator and cross-slits, 18×19 μm^2 at 195 m upstream of the end station, make the spatial coherence length of x-rays to be approximately 1 mm at the end station. An x-ray prism [9] was set so as to make its edge line vertical.

A cubic prism made of aclyric resin with 20 mm sides was inserted in the beam to deflect half of it [9, 10]. The x-ray glancing angle onto the prism and the deflection angle were 4 deg and 23 μrad ($\Delta\theta$). The direct and the refracted beams overlap with the width of 150 μm ($L_1\,\Delta\theta$) at 6.5 m (L_1) downstream of the prism where the photo cathode of x-ray zooming tube detector (modified C5333, Hamamatsu Photonics Co.) [11] was placed (Fig.1). The interference fringe spacing is 4 μm ($d=\lambda/(\Delta\theta)$). The deflection angle is chosen so as to compromise of the large interference region and the detectable fringe spacing. The detector has the magnification factor, the pixel size at the sample plane and the field of view of 55, 0.22 μm and 220 μmϕ. The measured spatial resolution of the detector was 0.7 μm at 8 keV [12]. The observed visibility of the fringes was 0.6.

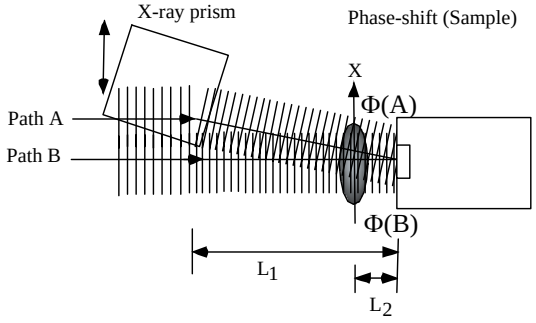

Figure 1: The schematic diagram of the two-beam shearing x-ray interferometer.

A sample was placed in front of the image detector by 96 mm (L_2). Interference signal between two slightly tilted beams are recorded with the detector. The phases of the two beams suffered local shifts in transmitting through the sample, causing a modulated interference pattern. The distance L_2 was close to the minimum possible due to the structure of the detector. The amount of shear was 2.2 μm ($L_2 \Delta\theta$) at the sample position. When Fresnel number, N_F (= $a^2/(\lambda L_2)$), is much greater than unity, the phase is easily retrieved without significant effect of Fresnel diffraction, where *a* is the sample structure size.

Samples observed are, (a) a Kapton foil (125 μmt with rough tapered edges, (b) a Nylon mesh (pitch 93 μm) and ascidian larvae (a biological specimen). The optical microscope images and the observed x-ray interference images (1 minute exposure) of the samples are shown in Fig.2. The upward / downward bents of the individual fringes were observed where the sample thickness has a positive / negative gradient in the downward direction (Fig.2(d)-(f)). Where the phase gradient of the samples are large ($\geqq 2\pi$ over the shear length), interference fringes appear discontinuous (e.g. along the lower Kapton foil edge in Fig.2(d)).

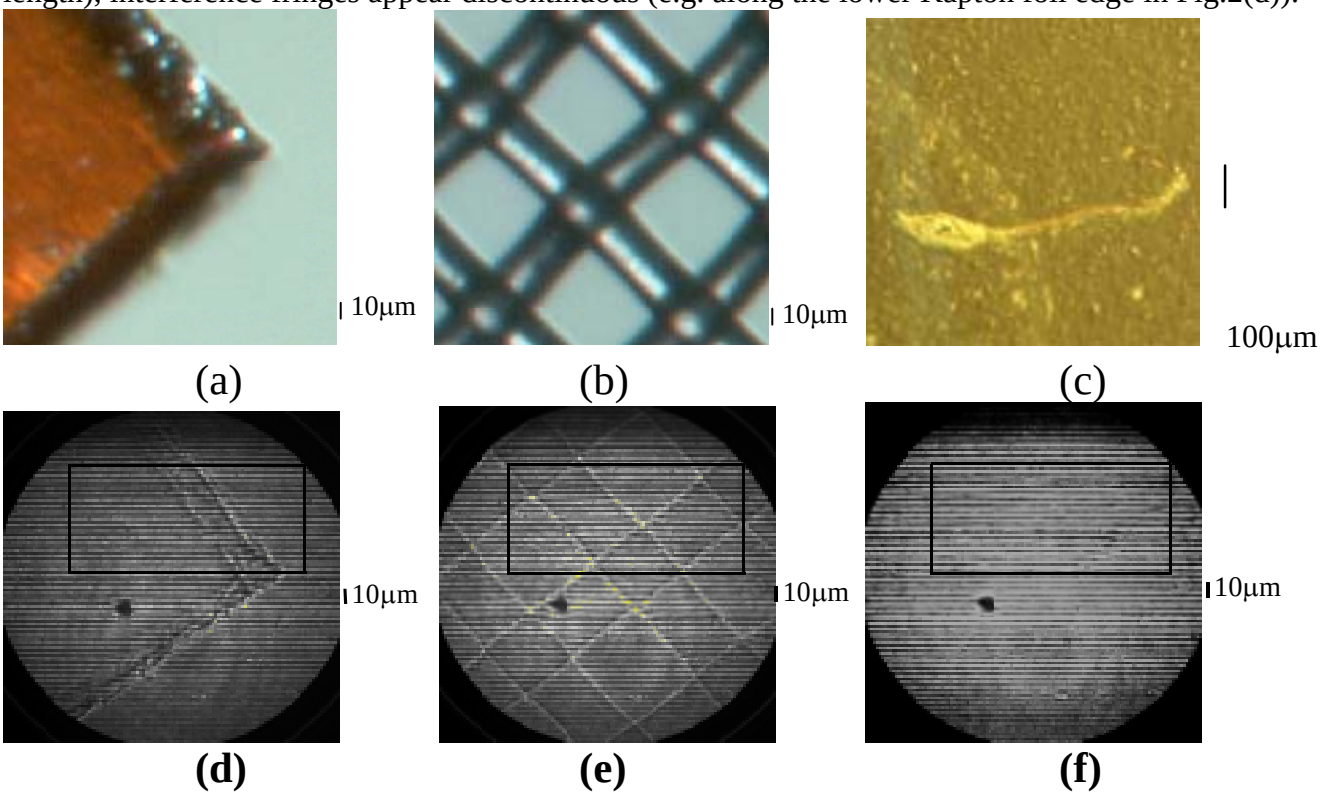

Figure 2: The visible microscope image for the samples (a) an edge of a Kapton foil (125 μmt), (b) a Nylon mesh (pitch 93 μm) and (c) an ascidian larvae (biological specimen). The observed x-ray interference images (d, e, f) for the samples (a, b, c).

2. EXPERIMENTAL RESULT

For the precise phase retrieval using the interferometers, the fringe scanning method [13] and the Fourier transform method [14] are widely used. We applied the fringe scanning method, since the higher spatial resolution close to that of the detector is easily achieved. For the phase shift in one of the optical paths the translational motion of the prism was introduced.

For the 4-step fringe scanning method, 0, 1/4π, 2/4π and 3/4π phase-shifts were given to path A by moving the prism by 0, 1/4*d*, 2/4*d* and 3/4*d* (where *d* is the fringe spacing). The intensity distributions at the detector plane, I_0, I_1, I_2 and I_3 were measured with and without the sample. The phase at the detector plane is calculated with the following equation, where $\Delta\phi$ is the differential phase due to the sample (similar equation is derived with $\Delta\phi=0$ for the dataset taken without the sample).

$$2\pi(k_A-k_B)(x)-\Delta\phi=\tan^{-1}((I_3-I_1)/(I_0-I_2)) \quad (1)$$

and

$$\Delta\phi=\phi(A)-\phi(B) \sim \delta\phi/\delta x\ (\Delta x) \quad (2),$$

where k_A-k_B are the X-ray wave-vectors along the path A and path B.

The phase distributions at the detector plane are calculated using eq.(1). Since the phase values calculated are the principal values from $-\pi/2$ to $\pi/2$, the phase unwrapping is carried out for the calculated phase distributions with and without the sample, independently. Subtraction between these two unwrapped phase gives the differential phase distribution of the sample without the complete knowledge of the carrier fringe. The differential phase of samples with various thickness gradient can be retrieved by adjusting the amount of shear.

The box areas in Fig.2(d)-(f) are analyzed. The calculated differential phase image for Fig.2(d) is shown in Fig.3(a). The areas where the thickness gradient is positive (negative) is shown in dark (bright) color. For the upper Kapton foil edge, the differential phase image shows almost monotonious thickness increase downward (Fig.3(a)). The measured differential phase for the upper Kapton edge is integrated along the line in Fig.3(a) and is shown in Fig.3(b). The derived phase due to the foil thickness was 15 rad (2.4 λ) close to the calculated value of 16 rad (2.5 λ), assuming the thickness of 125 μm and the index of refraction n=1- 2.0 $\times 10^{-6}$ at λ= 1 Å. The several horizontal lines in the differential phase images, in and out of the samples, are partly caused by the insufficient surface finish of the prism.

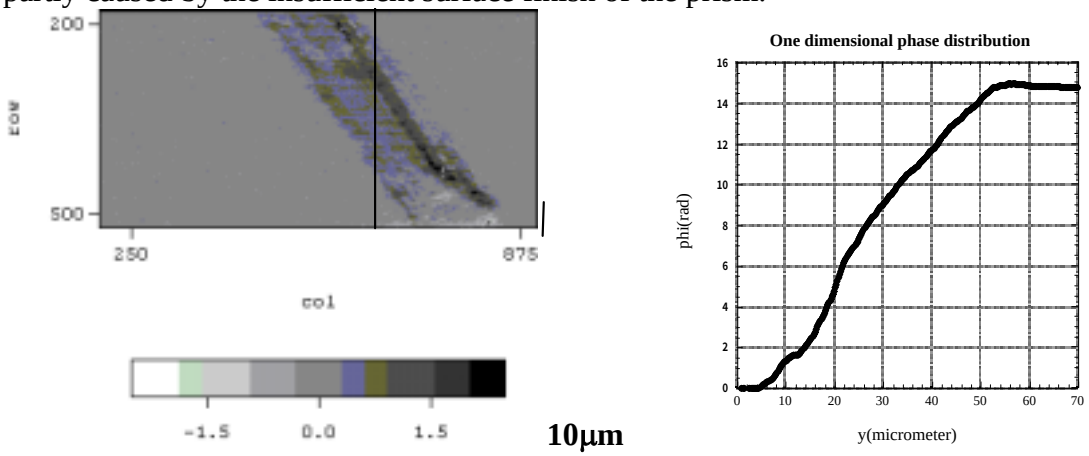

(a) **(b)**

Figure 3: The calculated differential phase (a) for the upper Kapton foil edge inside the region of interest in Fig.2(d) using the 4-step method and (b) The phase distribution of the upper Kapton foil edge by integrating the measured differential phase distribution.

Similar phase determination was done for one of the end of the nylon and an ascidian larva (almost transparent for the 1 Å X-ray) as shown in Fig.4(a) and (b), using 12-step method. In Fig.4(b), othoris, the gravity sensor with the diameter of about 10 μm is clearly observed.

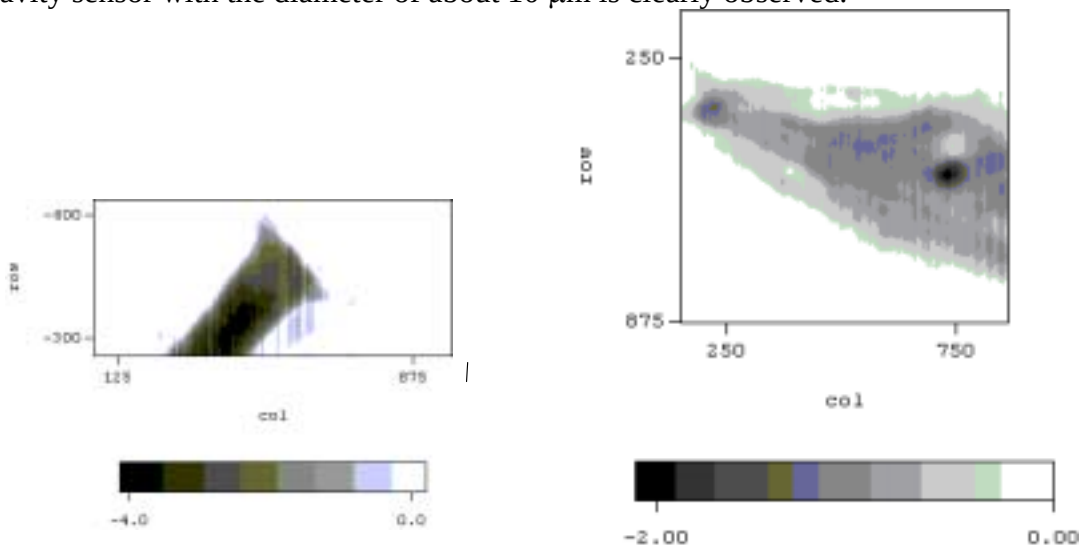

(a) (b)

Figure 4: The calculated phase (a) for the Nylon mesh and (b) for the ascidian larvae using the 12-step method.

3. IMPROVEMENT

To improve the precision of the phase retrieval, the surface of the X-ray prism needs to be improved. For this purpose, ultra precision cutting has been done on the surface of the acrylic resin using a single crystalline diamond tool which was developed at RIKEN. The surface roughness was evaluated to approximately 30 nm (RMS) with a Zygo NewView 200.

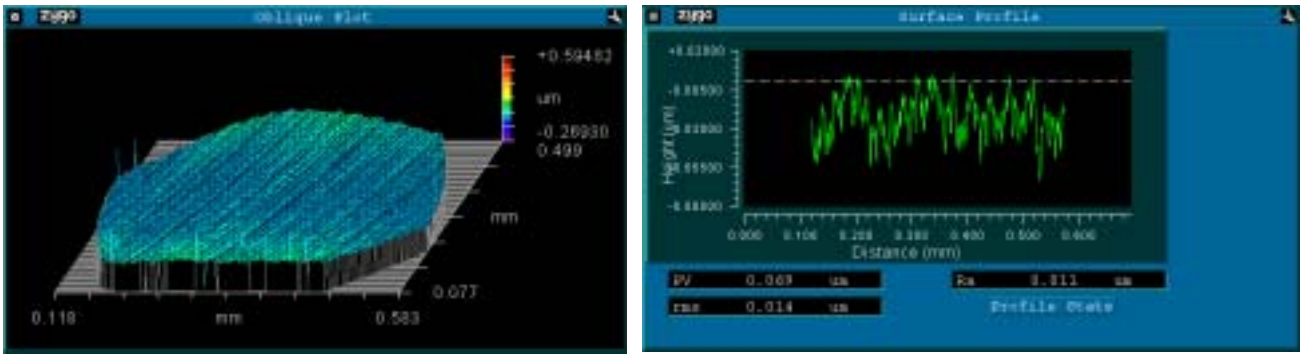

Figure 5:The surface roughness of improved acrylic X-ray prism evaluated with Zygo Newview200.

5. FUTURE PROSPECT

The present method is easily combined with the tomographic technique. The three dimensional refractive index distribution will be measured for visible-opaque and x-ray-weakly-absorbing samples with buried structures. Application of this new technique to material science, biological and medical sciences will be promising and fruitful.

References

1. J. Miao, P. Charalambous, J. Kirz, and D. Sayre, Nature (London), **400**, 342-344 (1999)
2. K. Siu, A.Y. Nikulin, K. Tamasaku, and T. Ishikawa, Applied Physics Letter, **79, 13**, 2112-2114 (2001)
3. K.A. Nugent, T.E. Gureyev, D.F. Cookson, D. Paganin, and Z. Barnea, Physical Review Letters, **77, 14**, 2961-2964 (1996)
4. P. Cloethens, W. Ludwig, J. Baruchel, D. Van Dyck, J. Van Landuyt, J.P. Guigay, and M. Schlenker, Applied Physics Letters, **75,19**, 2912-2914 (1999)
5. A. Momose, T. Takeda, Y. Itai, K. Hirano, Nature Medicine, **2, 4**, 473-475 (1996)
6. A. Momose, Nuclear Instruments and Methods in Physics Research, **A 352**, 622-628 (1995)
7. K.Iwata, H. Kikuta, H. Tadano, H. Hagino, and T. Nakano, Jpn. J. Appl. Phys., **38**, 6535-6539 (1999)
8. A.R. Lang, and A.P.W. Makepeace, Journal of Synchrotron Radiation, **6**, 59-61 (1999)
9. Y. Suzuki, Jpn. J. Appl. Phys. letter, **41**, **9AB**, 1019-1021 (2002)
10. Y. Kohmura, H.Takano, Y.Suzuki, T.Ishikawa, submitted to Applied Physics Letters (2002)
11. K. Kinoshita, T. Matsumura, Y. Inagaki, N. Hirai, M. Sugiyama, H. Kihara, N. Watanabe, and Y. Shimanuki, proc. of SPIE conference, **1741**, 287-293 (1992)
12. H. Takano, Y. Suzuki, K. Uesugi, A. Takeuchi, and N. Yagi, Proc. of the SPIE conference, **4499**, 126 (2001)
13. J.H. Bruning, D.R. Herriott, J.E. Gallagher, D.P. Rosenfeld, A.D. White, and D.J. Brangaccio, Appl. Optics, **13**, 2693 (1974)
14. M. Takeda, H. Ina, and S. Kobayashi, J. Opt. Soc. Am., **72**, 156-160 (1982)